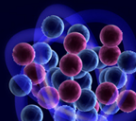


Effective Field Theory for Halo Nuclei

Chen Ji 计晨



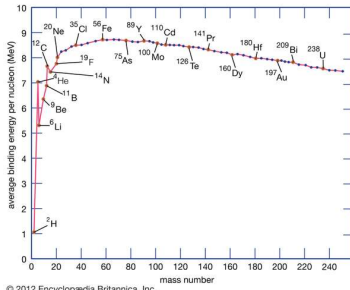
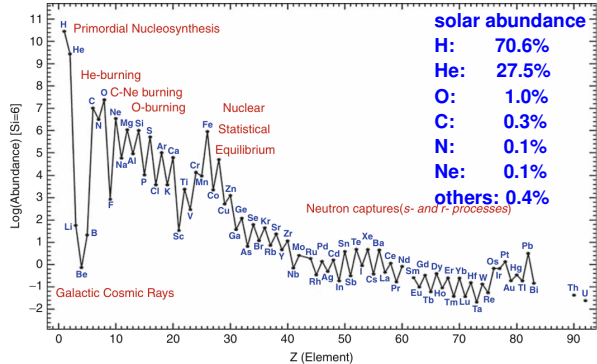
Central China Normal University
华中师范大学

The 17th Hadron Physics Online Forum (HAPOF)
Jan. 15, 2021

Outline

- Halo nuclei and nucleosynthesis
- Introduction to halo effective field theory
- EFT description of structure and reaction in halo nuclei
- Basic Concepts
 - EFT construction
 - Universal correlations in halo nuclei
 - Connect EFT with cluster models, ab initio theories, and experiments

Nuclear abundance and nucleosynthesis



● primordial/big-bang nucleosynthesis

Alpher, Bethe, Gamow ($\alpha\beta\gamma$)



Phys. Rev. 73 (1948) 803

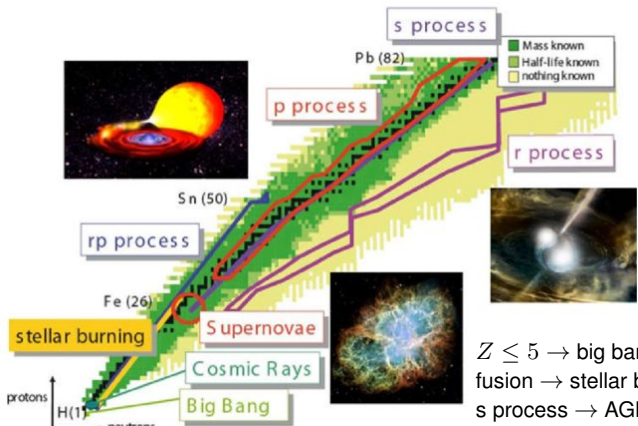
● stellar nucleosynthesis

Burbidge, Burbidge, Fowler, Hoyle (B²FH)



Rev. Mod. Phys. 29 (1957) 547

Nucleosynthesis & astrophysical processes



118 known elements

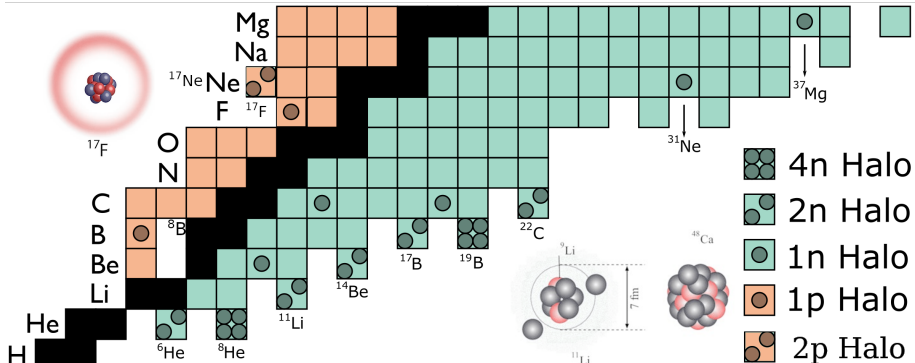
~3000 known isotopes

~4000 unknown isotopes

- $Z \leq 5 \rightarrow$ big bang / cosmic ray
- fusion \rightarrow stellar burning
- s process \rightarrow AGB star
- r process \rightarrow supernovae & neutron-star merger
- p & rp process \rightarrow sun-neutron-star binary

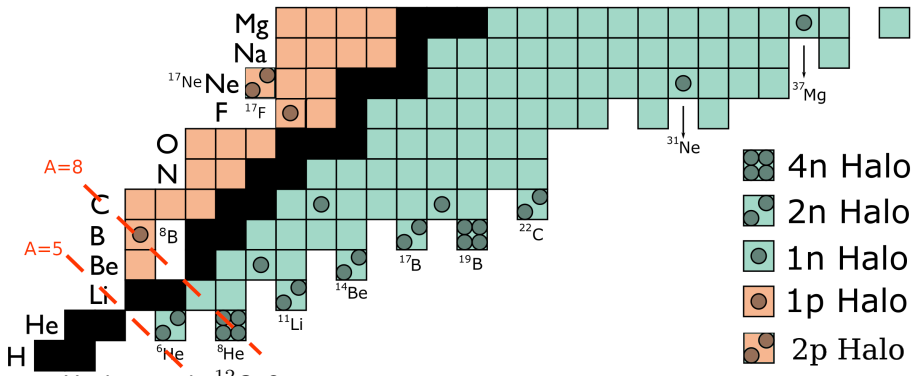
pic: Senger, Particles 3 (2020) 320

Halo nuclei

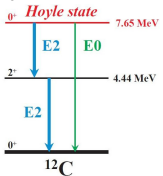
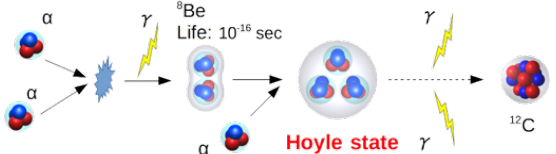


- far from stability (close to drip line)
- exhibit unique quantum features
 - light, p-rich or n-rich
 - bound/resonant states close to breakup threshold
- cluster structures
 - tight core surrounded loosely by valence nucleon(s)
 - large spatial extent
- enhanced cross section in astrophysical reaction at finite temperature

α cluster



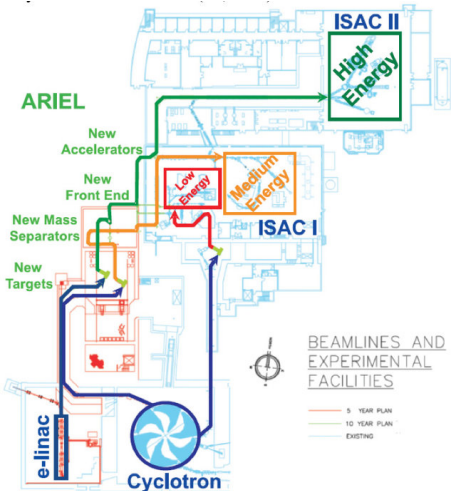
- Hoyle state in ^{12}C : 3α resonance
- triple- α reaction is enhanced by Hoyle state
- it bridges the gap between $A = 5$ and $A = 8$ in primordial nucleosynthesis



Exotic cluster/halo structures challenge experiments

Rare-Isotope Beam Facilities

- MSU-FRIB (USA)
- GANIL-SPIRAL2 (France)
- CERN-ISOLDE (EU)
- RIKEN-RIBF (Japan)
- TRIUMF-ISAC (Canada)
- HIRFL-RIBLL (China)
- GSI-FAIR (Germany) [construction]
- HIAF (China) [construction]
- RAON (Korea) [construction]
- BISOL (China) [plan]



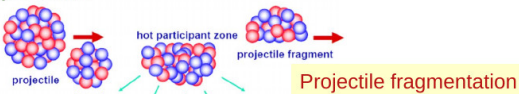
TRIUMF-ISAC

Production of rare isotopes

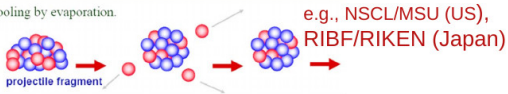
To produce dripline nuclei:

- In-flight fragmentation
 - heavy projectile
 - projectile fragmentation
 - 2nd beam > 25MeV
 - medium/high-Q reaction
- Isotopic separation on-line (ISOL)
 - light projectile
 - target fragmentation
 - 2nd beam ~ MeV
 - low-Q reaction
 - precision measurements
ISOTRAP, spectroscopy,
...

Random removal of protons and neutrons from heavy projectile in peripheral collisions



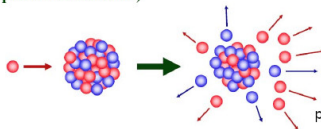
Cooling by evaporation.



Target fragmentation

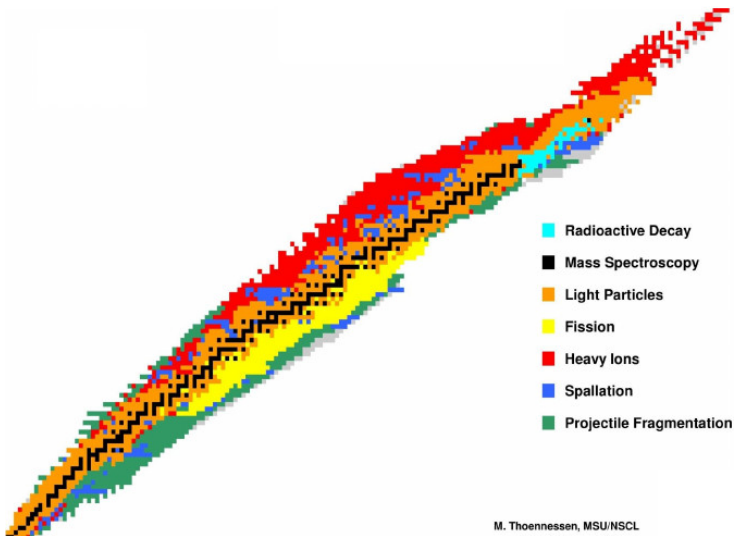
e.g., ISOLDE/CERN (Switzerland)
ISAC/TRIUMF (Canada), SPIRAL2
(France)

Random removal of protons and neutrons from heavy target nuclei by energetic light projectiles (pre-equilibrium and equilibrium emissions).



pic credit: A. Gade, MSU/FRIB

Production of rare isotopes

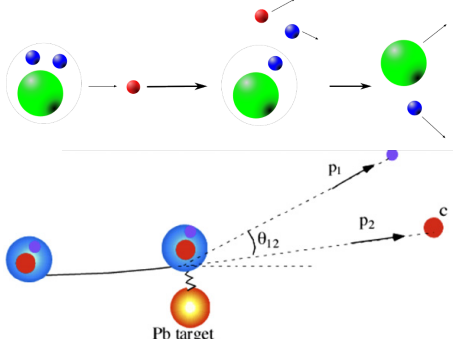
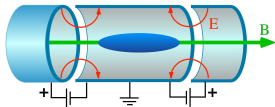


M. Thoennessen, MSU/NSCL

Experimental probes to halo nuclei

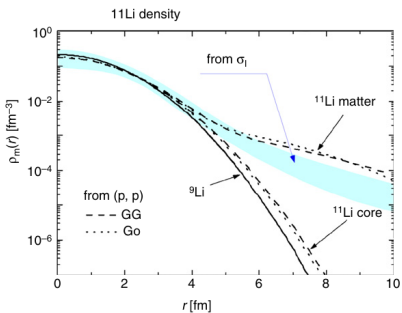
- static methods

- ISOTRAP: atomic mass
- laser spectroscopy: charge radius
- β -NMR: μ_M & Q_E



- reaction methods

- spectroscopy by breakup
 - nuclear breakup $p(^{11}\text{Li}, pn)^{10}\text{Li}$
 - Coulomb breakup $^{11}\text{Be}(\gamma^*, n)^{10}\text{Be}$
- spatial configuration
 - elastic scattering (p, p)
 - interaction cross section



review: Tanihata, Savajols, Kanungo, Prog. Part. Nucl. Phys. 68 (2013) 215

Halo nuclei challenge nuclear theories

- Three phases of halo theories
 - Back-of-the-envelope period (1985–1992)
 - “quick and dirty” estimates of halo properties by reproducing σ_R
 - gaussian spatial distribution → reproduce $\sigma_I \rightarrow R_m$ too small!
 - Few-body models period (1992–2000)
 - cluster structure models (core + valence nucleons)
 - few-body reaction models (Glauber, DWBA, CDCC,...)
 - unresolved model dependence
 - limited applicable regimes
 - Microscopic models period (2000–present)
 - ab initio structure theory
 - difficulties in computational power & extension to threshold physics
 - need to develop ab initio reaction theory (e.g. optical potential)
- Effective field theory (new era)
 - systematically embed microscopic information in cluster model
 - provide guidance to build reaction theory

Halo Nuclei, Al-Khalili, Morgan & Claypool Publishers, 2017

Introduction to effective field theory

Physics of Hadrons

Degrees of Freedom



quarks, gluons

Energy (MeV)

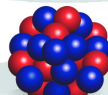
940
neutron mass

constituent quarks



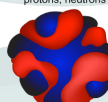
baryons, mesons

140
pion mass



protons, neutrons

8
proton separation energy in lead



nucleonic densities
and currents

1.12
vibrational state in tin



collective coordinates

0.043
rotational state in uranium

scale hierarchy in nuclear physics

Physics of Nuclei

Introduction to effective field theory

Physics of Hadrons

Degrees of Freedom

Energy (MeV)



quarks, gluons



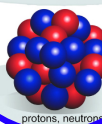
constituent quarks

940
neutron mass



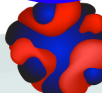
baryons, mesons

140
pion mass



protons, neutrons

8
proton separation energy in lead



nucleonic densities and currents

1.12
vibrational state in tin



collective coordinates

0.043
rotational state in uranium

scale hierarchy in nuclear physics

underlying theory

high scale: Λ

low scale: Q

Introduction to effective field theory

Physics of Hadrons

Degrees of Freedom

Energy (MeV)



quarks, gluons



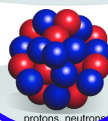
constituent quarks

940
neutron mass



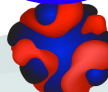
baryons, mesons

140
pion mass



protons, neutrons

8
proton separation energy in lead



nucleonic densities
and currents

phenomeno-
logical theory

high scale: Λ

low scale: Q

underlying theory

1.12
vibrational state in tin

0.043
rotational state in uranium

collective coordinates

Introduction to effective field theory

Physics of Nuclei

Degrees of Freedom

Energy (MeV)



quarks, gluons



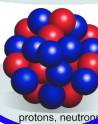
constituent quarks

940
neutron mass



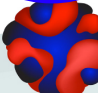
baryons, mesons

140
pion mass



protons, neutrons

8
proton separation energy in lead



nucleonic densities
and currents

1.12
vibrational state in tin



collective coordinates

0.043
rotational state in uranium

scale hierarchy in nuclear physics

underlying theory

high scale: Λ

low scale: Q

phenomeno-
logical theory

effective field
theory

- EFT emerges from underlying theory
- EFT “inherits” asymptotics from phenomenology

Key elements of an EFT

- Separation of scales $Q \ll \Lambda$:
 - low-energy observables $\rightarrow Q$
 - short-range interactions $\rightarrow \Lambda$

Key elements of an EFT

- Separation of scales $Q \ll \Lambda$:
 - low-energy observables $\rightarrow Q$
 - short-range interactions $\rightarrow \Lambda$
- Systematic expansion of Lagrangian in Q/Λ :
 - order-by-order construction of effective interactions:

$$V_{\text{eff}} = \sum_n \hat{V}^{(n)}; \quad \hat{V}^{(n)} \sim (Q/\Lambda)^{n-1}$$

- prediction uncertainty is controlled by $(Q/\Lambda)^{(n+1)}$

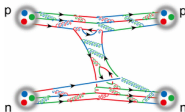
Key elements of an EFT

- Separation of scales $Q \ll \Lambda$:
 - low-energy observables $\rightarrow Q$
 - short-range interactions $\rightarrow \Lambda$
- Systematic expansion of Lagrangian in Q/Λ :
 - order-by-order construction of effective interactions:
$$V_{\text{eff}} = \sum_n \hat{V}^{(n)}; \quad \hat{V}^{(n)} \sim (Q/\Lambda)^{n-1}$$
 - prediction uncertainty is controlled by $(Q/\Lambda)^{(n+1)}$
- Predict low-energy physics:
 - low-energy observables (Q) insensitive details of short-range interactions (Λ)
 - EFT unveils universal correlations

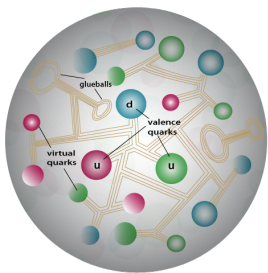
NN interaction in atomic nuclei

$\Lambda \sim 1\text{ GeV}$

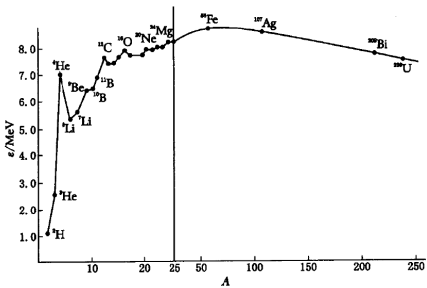
QCD



$Q \sim 100\text{ MeV}$



Λ : EFT breakdown scale

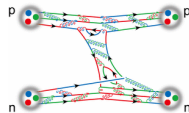
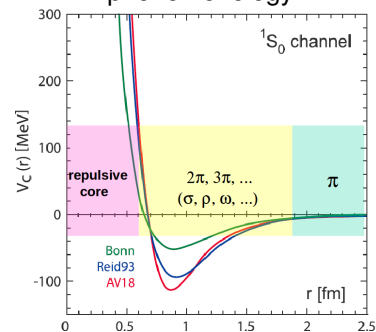


$Q \approx \sqrt{2M_N B/A}$: typical scale in EFT

NN interaction in atomic nuclei

$\Lambda \sim 1\text{ GeV}$

$Q \sim 100\text{ MeV}$  phenomenology

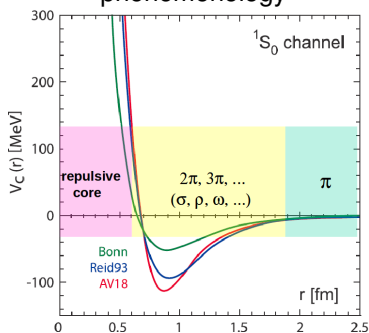


pic: Aoki et al. Comp. Sci. Disc. 2008

NN interaction in atomic nuclei

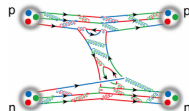
$\Lambda \sim 1 \text{ GeV}$

$Q \sim 100 \text{ MeV}$
 phenomenology

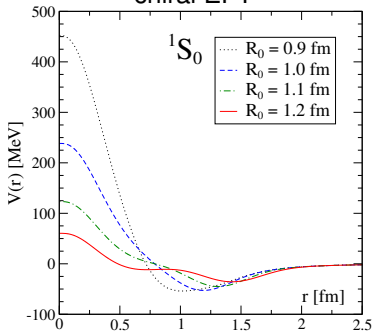


pic: Aoki et al. Comp. Sci. Disc. 2008

QCD



chiral EFT



pic: Gezerlis et al. Phys. Rev. C 2014

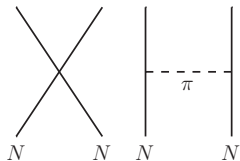
EFT with contact interactions

- Effective field theory with contact interactions originate from pionless EFT

chiral EFT NN force

- short range: $V_s = C_0$
- intermediate/long range:

$$V_{1\pi} \sim \frac{1}{q^2 + m_\pi^2}$$



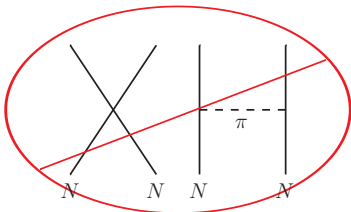
EFT with contact interactions

- Effective field theory with contact interactions originate from pionless EFT

chiral EFT NN force

- short range: $V_s = C_0$
- intermediate/long range:

$$V_{1\pi} \sim \frac{1}{q^2 + m_\pi^2}$$



\not EFT NN force

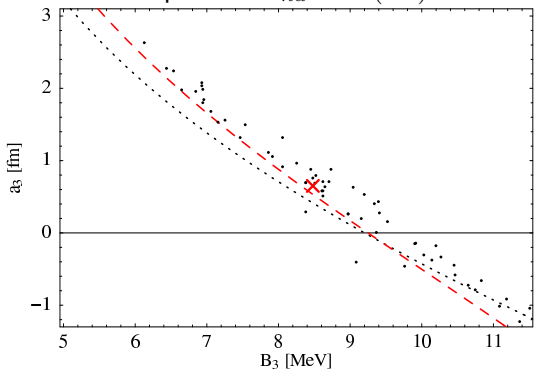
- NN momentum $q^2 \ll m_\pi^2$

$$V_{1\pi} \xrightarrow{q^2 \ll m_\pi^2} C_0 + C_2 q^2 + \dots$$

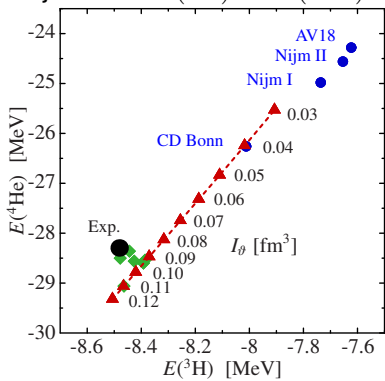


Universality in $\not\! EFT$

Phillips Line: a_{nd} vs $B(^3H)$



Tjon Line: $B(^3H)$ vs $B(^4He)$

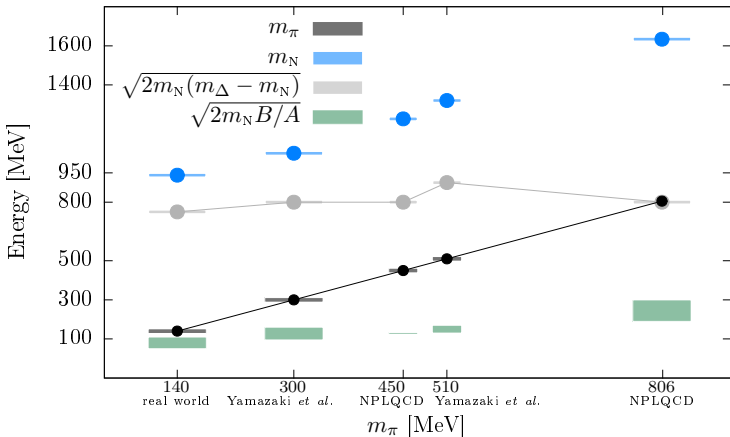


- $\not\! EFT$ indicates universal correlations among few-body observables
- long-range (low-energy) physics is insensitive to details of short-range interactions

EFT with contact interactions

- Lattice simulated nuclei

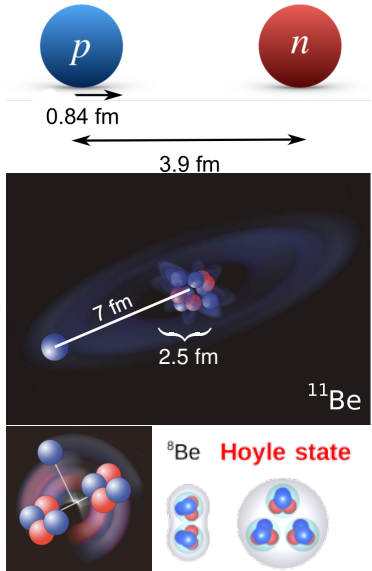
- $M_\pi \gg 140 \text{ MeV}; Q = \sqrt{2M_N B/A} \ll m_\pi$



Nuclear halo and cluster

few-body molecular structure

- ^2H
- simplest neutron halo
- neutron halos
 - $^6\text{He}, ^{11}\text{Be}, \dots$
- proton halos
 - $^{17}\text{F}^*, ^8\text{B}$
- α -clustering
 - $^9\text{Be}: \alpha + \alpha + n$
 - $^8\text{Be}, ^{12}\text{C}^*$

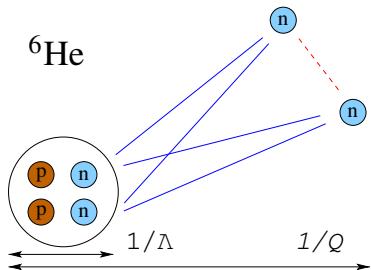


Halo physics near clustering threshold

$$\Lambda \sim \sqrt{m_N E_{\text{core}}^*}$$

ab initio theory

$$Q \sim \sqrt{m_N S_N}$$



Halo physics near clustering threshold

$$\Lambda \sim \sqrt{m_N E_{\text{core}}^*}$$

ab initio theory

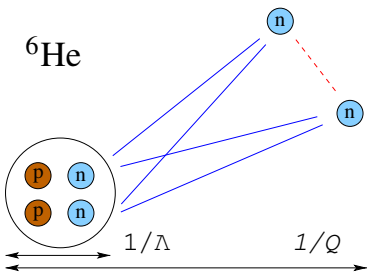
$$Q \sim \sqrt{m_N S_N}$$

halo physics is difficult for ab initio theories

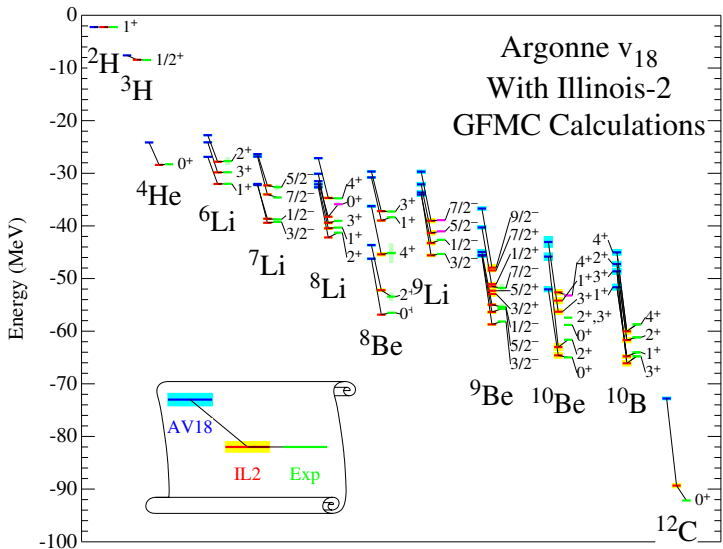
- continuum problem in many-body calculations
NCSMC, GSM-Bergren, Lattice-EFT, LIT, ...
- uncertainty control in chiral potentials
threshold observable converges slower in χ EFT

halo scale : $Q_{\text{halo}} \ll Q_{\chi\text{EFT}} \approx (2M_N B/A)^{1/2}$

uncertainty : $\Delta_{\text{halo}} \% \approx \frac{Q_{\chi\text{EFT}}}{Q_{\text{halo}}} \left(\frac{Q_{\chi\text{EFT}}}{\Lambda_{\chi\text{EFT}}} \right)^{(n+1)}$



ab initio description of nuclear spectrum



microscopic description of nuclear spectrum is in general accurate

ab initio description of halo features

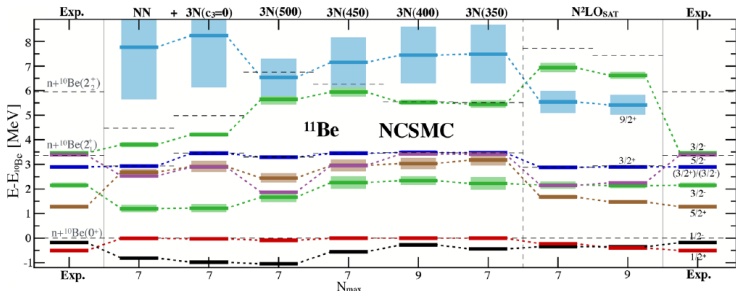
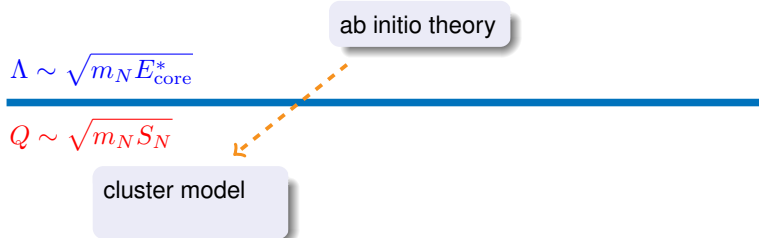


FIG. 2. NCSMC spectrum of ^{11}Be with respect to the $n + ^{10}\text{Be}$ threshold. Dashed black lines indicate the energies of the ^{10}Be states. Light boxes indicate resonance widths. Experimental energies are taken from Refs. [1,51].

- ab initio calculation of ^{11}Be has been done by NCSMC
- predictions of threshold properties rely significantly on the nuclear interactions

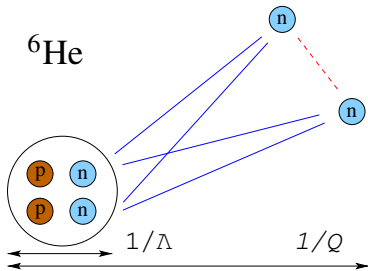
Calci et al. Phys. Rev. Lett. 117 (2016) 242501

Halo physics near clustering threshold



difficulties in cluster models:

- assess model dependence?
- assign theory uncertainty



Halo physics near clustering threshold

$$\Lambda \sim \sqrt{m_N E_{\text{core}}^*}$$

$$Q \sim \sqrt{m_N S_N}$$

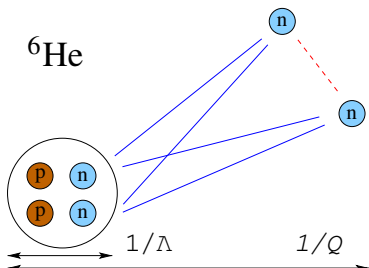
ab initio theory

cluster model

halo EFT



- cluster configuration in halo EFT:
core + valence nucleons d.o.f.
- separation of scales:
 $Q \ll \Lambda \rightarrow$ systematic expansion in observables
- short-range physics from underlying theory:
anti-symmetrization of core nucleons is embedded
in contact interactions



Halo Effective Field Theory

- We adopt EFT with contact interactions to describe clustering in halo nuclei
- introduce auxiliary two-body fields for bound/resonance states

$$\mathcal{L} = \mathcal{L}_1 + \mathcal{L}_2 + \mathcal{L}_3$$

$$\mathcal{L}_1 = n^\dagger \left(i\partial_0 + \frac{\nabla^2}{2m_n} \right) n + c^\dagger \left(i\partial_0 + \frac{\nabla^2}{2m_c} \right) c$$

$$\begin{aligned}\mathcal{L}_2 = & s^\dagger \left[\eta_0 \left(i\partial_0 + \frac{\nabla^2}{4m_n} \right) + \Delta_0 \right] s + \sigma^\dagger \left[\eta_1 \left(i\partial_0 + \frac{\nabla^2}{2(m_n + m_c)} \right) + \Delta_1 \right] \sigma \\ & + g_0 [s^\dagger(nn) + \text{h.c.}] + g_1 [\sigma^\dagger(nc) + \text{h.c.}],\end{aligned}$$

$$\mathcal{L}_3 = h (\sigma n)^\dagger (\sigma n)$$

- 2-body contact (LO)

A horizontal black line representing a particle exchange splits into two diagonal lines representing particles. This represents a contact interaction between two particles.

$$= -i\sqrt{2}g$$

$g \leftarrow$ 2-body observable

- 3-body contact (LO)

A horizontal black line representing a particle exchange splits into three diagonal lines representing particles. This represents a contact interaction involving three particles.

$$= ih$$

$h \leftarrow$ 3-body observable

One-neutron s-wave halos

- scattering amplitude: $t_0(k) = \frac{2\pi}{\mu} \left(\frac{1}{a_0} - \frac{r_0}{2} k^2 + ik \right)^{-1}$

- in low-energy bound/virtual state: $a_0 \sim 1/Q$; $r_0 \sim 1/\Lambda$
- expand t-matrix in r_0/a_0

One-neutron s-wave halos

scattering amplitude: $t_0(k) = \frac{2\pi}{\mu} \left(\frac{1}{a_0} - \frac{r_0}{2} k^2 + ik \right)^{-1}$

- in low-energy bound/virtual state: $a_0 \sim 1/Q$; $r_0 \sim 1/\Lambda$
- expand t-matrix in r_0/a_0

Iterative summation at LO



One-neutron s-wave halos

- scattering amplitude: $t_0(k) = \frac{2\pi}{\mu} \left(\frac{1}{a_0} - \frac{r_0}{2} k^2 + ik \right)^{-1}$
 - in low-energy bound/virtual state: $a_0 \sim 1/Q$; $r_0 \sim 1/\Lambda$
 - expand t-matrix in r_0/a_0
- Iterative summation at LO

- tune coupling

- LO: $a_0 = \left(\frac{2\pi\Delta}{\mu g^2} + \Lambda \right)^{-1}$
- NLO: $r_0 = -\eta \frac{2\pi}{\mu^2 g^2}$

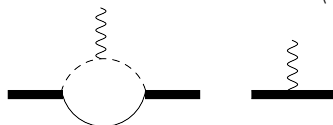
One-neutron s-wave halos

- scattering amplitude: $t_0(k) = \frac{2\pi}{\mu} \left(\frac{1}{a_0} - \frac{r_0}{2} k^2 + ik \right)^{-1}$
 - in low-energy bound/virtual state: $a_0 \sim 1/Q$; $r_0 \sim 1/\Lambda$
 - expand t-matrix in r_0/a_0
- Iterative summation at LO
- tune coupling
 - LO: $a_0 = \left(\frac{2\pi\Delta}{\mu g^2} + \Lambda \right)^{-1}$
 - NLO: $r_0 = -\eta \frac{2\pi}{\mu^2 g^2}$
- pole expansion: $t_0(k) \approx \frac{2\pi}{\mu} \frac{\mathcal{Z}_R}{\gamma_0 + ik}$
 - ANC: $\psi_0(\mathbf{r}) = \frac{C_\sigma}{\sqrt{4\pi r}} \exp(-\gamma_{0,\sigma} r)$
 - LO: $C_{\sigma,LO} = \sqrt{2\gamma_0}$
 - NLO: $C_{\sigma,NLO} = \sqrt{\frac{2\gamma_0}{1 - \gamma_0 r_0}}$
 - renormalization constant $\mathcal{Z}_R = \frac{C_{\sigma,NLO}^2}{C_{\sigma,LO}^2} = \frac{1}{1 - \gamma_0 r_0}$

One-neutron s-wave halos

	^2H	^{11}Be	^{15}C	^{19}C
Experiment				
S_{1n} [MeV]	2.224573(2)	0.50164(25)	1.2181(8)	0.58(9)
E_c^* [MeV]	140	3.36803(3)	6.0938(2)	1.62(2)
$\langle r_{nc}^2 \rangle^{1/2}$ [fm]	3.936(12)	6.05(23)	4.15(50)	6.6(5)
	3.95014(156)	5.7(4)	7.2±4.0	6.8(7)
		5.77(16)	4.5(5)	5.8(3)
Halo EFT				
Q/Λ	0.33	0.39	0.45	0.6
r_0/a_0	0.32	0.32	0.43	0.33
$\sqrt{\mathcal{Z}_R}$	1.295	1.3	1.63	1.3
$\langle r_{nc}^2 \rangle^{1/2}$ [fm]	3.954	6.85	4.93	5.72

Electric form factor → radius $\langle r_{nc}^2 \rangle^{1/2}$

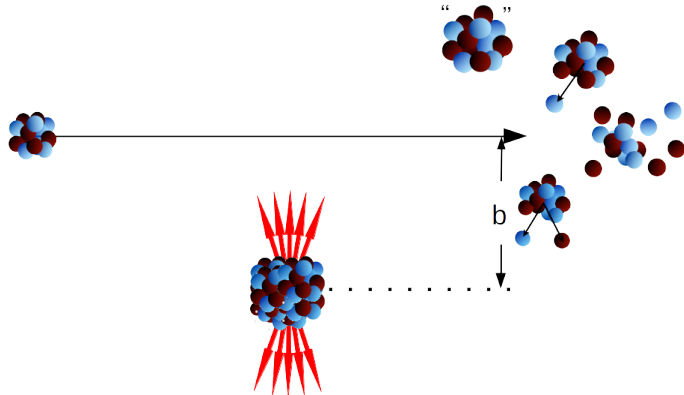


$$F_{nc}(q^2) = \mathcal{Z}_R \frac{2\gamma_0}{q} \arctan\left(\frac{q}{2\gamma_0}\right) + 1 - \mathcal{Z}_R$$

$$F_{nc}(q^2) = 1 - \frac{1}{6} \langle r_{nc}^2 \rangle q^2 + \mathcal{O}(q^4),$$

Coulomb dissociation in $1n$ halos

- Coulomb dissociation
 - breakup by colliding a halo nucleus with a high-Z nucleus
 - the halo dynamics dominates when $E_\gamma \sim S_{1n}$

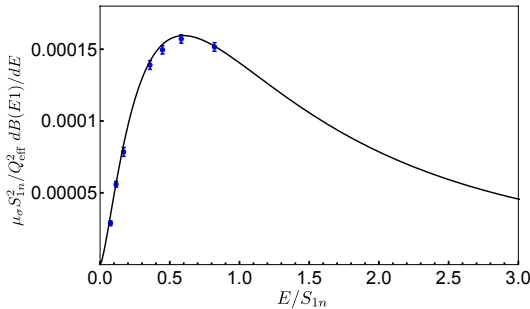


EFT on Coulomb dissociation

- E1 transition



$$\frac{dB(E1)}{dE_\gamma} = \frac{1}{(2\pi)^3} \left(|\mathcal{M}_{E1}^{(J=1/2)}|^2 + |\mathcal{M}_{E1}^{(J=3/2)}|^2 \right) \frac{d^3 p}{dE_\gamma} = \frac{\mathcal{Z}_R Q_{\text{eff}}^2}{\mu_{nc} S_{1n}^2} \frac{3\alpha_{em}}{\pi^2} \frac{(E_\gamma/S_{1n})^{3/2}}{(E_\gamma/S_{1n} + 1)^4}.$$

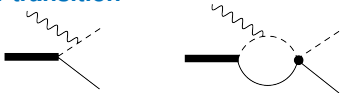


deuteron E1 strength

Hammer, CJ, Phillips, JPG 44 (2017) 103002

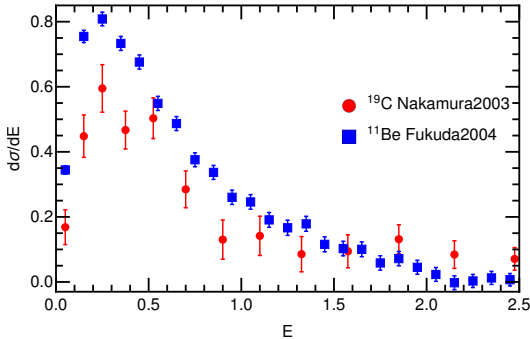
EFT on Coulomb dissociation

- E1 transition



$$\frac{d\sigma}{dE_\gamma} = \frac{16\pi^3}{9} N_{E1}(E_\gamma, R)$$

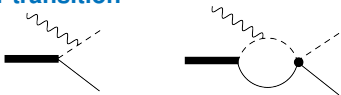
$$\frac{dB(E1)}{dE_\gamma}$$



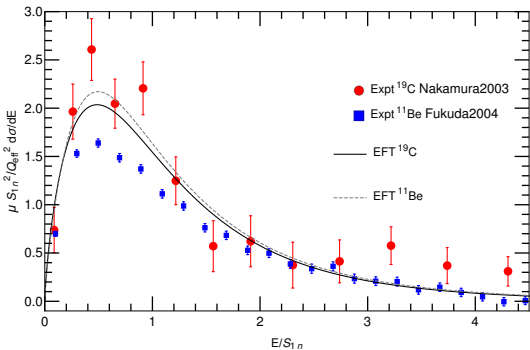
Coulomb dissociation energy spectrum in
 ^{11}Be and ^{19}C

EFT on Coulomb dissociation

- E1 transition



$$\frac{\mu_{nc} S_{1n}^2}{Z_R Q_{\text{eff}}^2} \frac{d\sigma}{dE_\gamma} = \frac{16\pi^3}{9} N_{E1}(E_\gamma, R) \frac{\mu_{nc} S_{1n}^2}{Z_R Q_{\text{eff}}^2} \frac{dB(\text{E1})}{dE_\gamma}$$



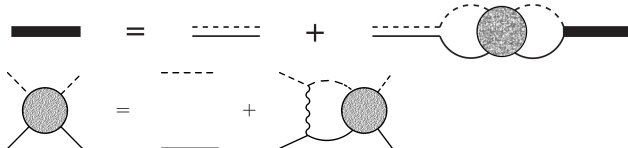
Coulomb dissociation energy spectrum in
 ^{11}Be and ^{19}C \rightarrow Universality!

^{11}Be : fit ANC in NCSMC [Calci et al. '16]

Hammer, Phillips, NPA '11
Acharya, Phillips, NPA '13
Hammer, CJ, Phillips, JPG '17

Halo EFT with Coulomb

- In halo/clustering systems with Coulomb interactions, a new scale $k_c = Q_c \alpha_{em} \mu$ enters
 - $k_c \gtrsim Q$: Coulomb interaction is nonperturbative



- Coulomb Green's function (non-perturbative)

$$(\mathbf{r}|G_C(E)|\mathbf{r}') = \int \frac{d^3 p}{(2\pi)^3} \frac{\psi_{\mathbf{p}}(\mathbf{r})\psi_{\mathbf{p}}^*(\mathbf{r}')}{E - \mathbf{p}^2/(2\mu_{nc}) + i\epsilon}$$

$$\psi_{\mathbf{p}}(\mathbf{r}) = \sum_{l=0}^{\infty} (2l+1) i^l \exp(i\sigma_l) \frac{F_l(\eta, \rho)}{\rho} P_l(\hat{\mathbf{p}} \cdot \hat{\mathbf{r}})$$

p - p scattering [Kong, Ravndal, PLB '99; NPA '10]

p - α and α - α scattering [Higa, Hammer, van Kolck, NPA '08; Higa, FBS '11]

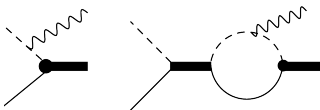
$^{17}\text{F}^*$ [Ryberg, Forssén, Hammer, Platter, PRC '14; AnnPhys '16]

- $k_c \ll Q$: Coulomb interaction is perturbative

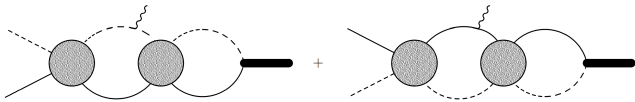
^3H and ^3He [König, Grießhammer, Hammer, van Kolck, JPG '16]

Radiative Nucleon Captures

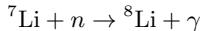
neutron captures



proton captures

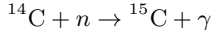


$$\frac{d\sigma}{d\Omega} = \frac{\mu_{nc} E_\gamma}{8\pi^2 p} \sum_{i=1}^2 \left| \epsilon_i \cdot \frac{\mathcal{M}}{\sqrt{\Sigma'(-B)}} \right|^2$$

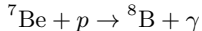


Rupak, Higga, PRL '11; Fernando, Higa, Rupak, EPJA '12;

Zhang, Nollett, Phillips, PRC '14



Rupak, Fernando, Vaghani, PRC '12



Zhang, Nollett, Phillips, PRC '14; Ryberg, et al. EPJA '14



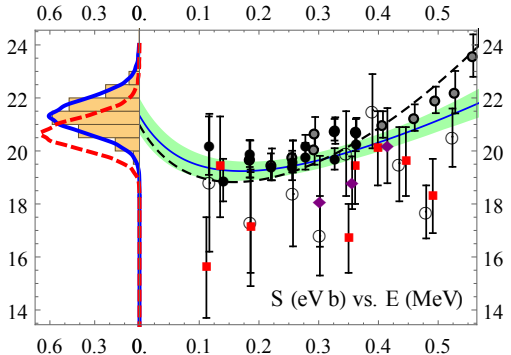
Ryberg, Forssén, Hammer, Platter, PRC '14; AnnPhy '16

Radiative Nucleon Captures

astrophysical S-factor for ${}^7\text{Be}(p, \gamma){}^8\text{B}$

EFT(NLO): VMC ANC + Bayesian error analysis

Zhang, Nollett, Phillips, Phys. Lett. B 751 (2015) 535

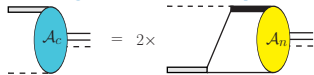


$$S(E) = E e^{2\pi\eta(E)} \sigma(E)$$

$$S(0) = 21.3 \pm 0.7 \text{ eV} \cdot \text{b}$$

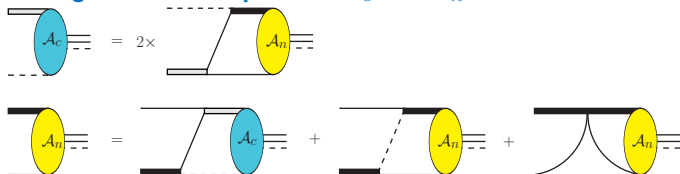
$2n$ halos in Faddeev formalism

- solving transition amplitudes \mathcal{A}_c and \mathcal{A}_n



$2n$ halos in Faddeev formalism

- solving transition amplitudes \mathcal{A}_c and \mathcal{A}_n



- three-body wave functions

$$\Psi_n(\mathbf{p}, \mathbf{q}) = \begin{array}{c} \text{---} \\ \text{---} \\ \text{---} \end{array} \begin{array}{c} \text{---} \\ \text{---} \\ \text{---} \end{array} \begin{array}{c} \text{---} \\ \text{---} \\ \text{---} \end{array} + \begin{array}{c} \text{---} \\ \text{---} \\ \text{---} \end{array} \begin{array}{c} \text{---} \\ \text{---} \\ \text{---} \end{array} \begin{array}{c} \text{---} \\ \text{---} \\ \text{---} \end{array} + \begin{array}{c} \text{---} \\ \text{---} \\ \text{---} \end{array} \begin{array}{c} \text{---} \\ \text{---} \\ \text{---} \end{array} \begin{array}{c} \text{---} \\ \text{---} \\ \text{---} \end{array}$$

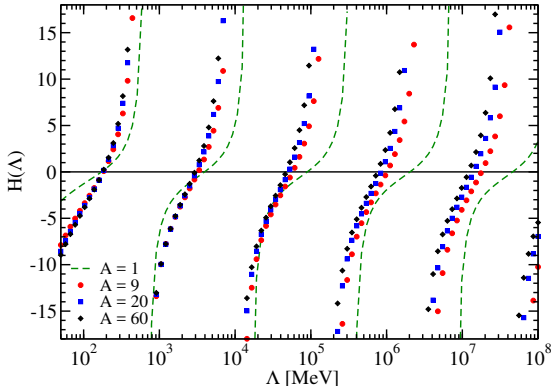
Diagram showing the three-body wave function $\Psi_n(\mathbf{p}, \mathbf{q})$ as a sum of three terms. Each term consists of a horizontal line with a vertical dashed line segment, followed by a yellow oval, followed by a horizontal line with a vertical dashed line segment.

$$\Psi_c(\mathbf{p}, \mathbf{q}) = \begin{array}{c} \text{---} \\ \text{---} \\ \text{---} \end{array} \begin{array}{c} \text{---} \\ \text{---} \\ \text{---} \end{array} \begin{array}{c} \text{---} \\ \text{---} \\ \text{---} \end{array} + 2 \times \begin{array}{c} \text{---} \\ \text{---} \\ \text{---} \end{array} \begin{array}{c} \text{---} \\ \text{---} \\ \text{---} \end{array} \begin{array}{c} \text{---} \\ \text{---} \\ \text{---} \end{array}$$

Diagram showing the three-body wave function $\Psi_c(\mathbf{p}, \mathbf{q})$ as a sum of two terms. The first term is similar to the Ψ_n diagram. The second term is identical to the first but preceded by a factor of 2.

Three-body renormalization

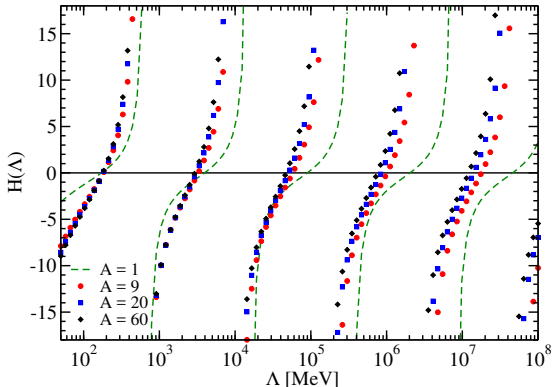
- running of three-body coupling
 - tune $H(\Lambda) = \Lambda^2 h / 2mg^2$:
 - reproduce one observable in a $2n$ -halo



Hammer, CJ, Phillips,
JPG 44 (2017) 103002

Three-body renormalization

- running of three-body coupling
 - tune $H(\Lambda) = \Lambda^2 h / 2mg^2$:
reproduce one observable in a $2n$ -halo
 - $H(\Lambda)$ periodic for $\Lambda \rightarrow \lambda\Lambda$ [$A = 1$ Bedaque *et al.* '00]



Hammer, CJ, Phillips,
JPG 44 (2017) 103002

Three-body renormalization

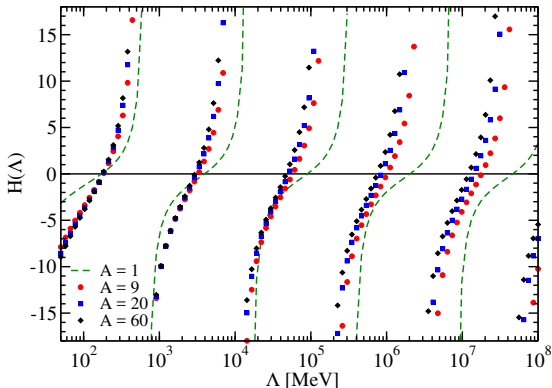
- running of three-body coupling

- tune $H(\Lambda) = \Lambda^2 h / 2mg^2$:
reproduce one observable in a $2n$ -halo

- $H(\Lambda)$ periodic for $\Lambda \rightarrow \lambda\Lambda$ [$A = 1$ Bedaque *et al.* '00]

- $H(\Lambda)$ appears as RG limit cycle [Mohr *et al.*, AnnPhys '06]

- discrete scale invariance → Efimov physics



Hammer, CJ, Phillips,
JPG 44 (2017) 103002

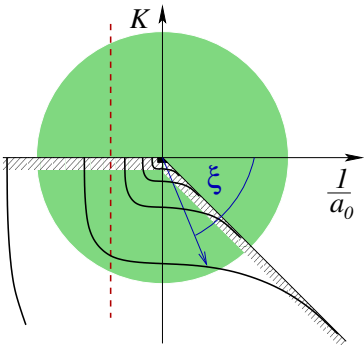
Efimov physics

- a universal spectrum of three-body bound states

$$B_3 = -\frac{1}{ma_0^2} + [e^{-2\pi n} f(\xi)]^{1/s_0} \frac{\kappa_*^2}{m}$$

Braaten, Hammer, Phys. Rept. '06

- atomic physics: vary a_0 through Feshbach resonance
- nuclear physics: fixed a_0



Efimov physics

- a universal spectrum of three-body bound states

$$B_3 = -\frac{1}{ma_0^2} + [e^{-2\pi n} f(\xi)]^{1/s_0} \frac{\kappa_*^2}{m}$$

Braaten, Hammer, Phys. Rept. '06

- atomic physics: vary a_0 through Feshbach resonance
- nuclear physics: fixed a_0

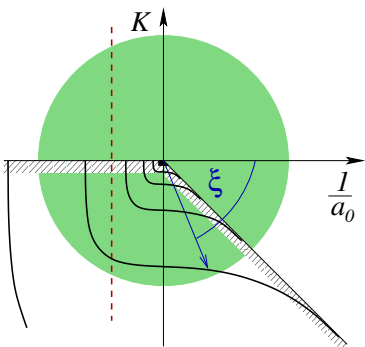
- unitary limit ($a \rightarrow \infty$):

$$B_3 = e^{-2\pi n/s_0} \frac{\kappa_*^2}{m}$$

- discrete scale invariance:

$$\kappa_* \rightarrow \kappa_*, \quad a_0 \rightarrow e^{\pi n/s_0} a_0$$

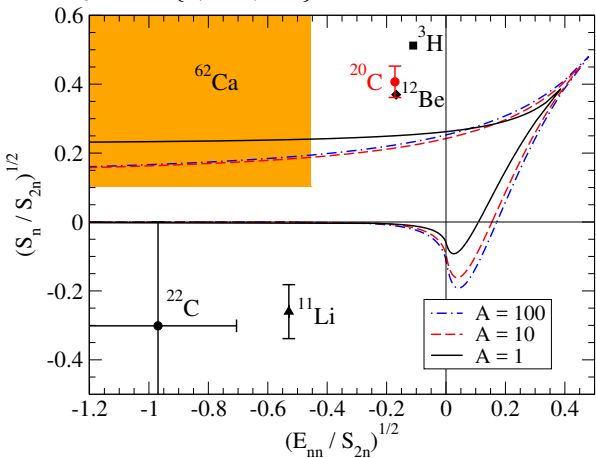
- exploring Efimov physics in halo nuclei is an important subject



Efimov universality in $2n$ s-wave halo

- contour constraints on ground-state energy S_{2n} if the excited-state energy

$$B_3^* = \max\{0, E_{nn}, S_{1n}\}$$



Canham, Hammer, EPJA '08; Frederico *et al.* PPNP '12;

Hammer, CJ, Phillips, JPG 44 (2017) 103002

^{22}C : $2n$ Halo

	^{20}C	^{21}C	^{22}C
bound/unbound	bound	unbound	bound
ground state	0^+	$S_{1/2}$	0^+
binding/virtual energy [MeV]	$S_{1n}: 2.93(26)$ AME2012	$S_{1n}: -0.01(47)$ AME2012	$S_{2n}: 0.11(6)$ AME2012
matter radius r_m [fm]	$2.97^{+0.03}_{-0.05}$ Togano et al. '16	< -2.9 Mosby et al. '13	$S_{2n}: -0.14(46)$ Gaudefroy et al. '12

- Halo EFT

we fit to ^{22}C matter radius to constrain:

- S_{1n} in ^{21}C ($a < 0$)
- S_{2n} in ^{22}C

Correlations in ^{22}C

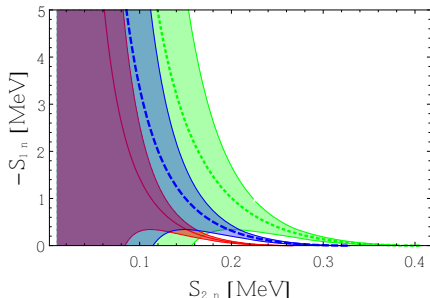
$$\langle r_m^2 \rangle_{2n\text{-halo}} - \frac{A}{A+2} \langle r_m^2 \rangle_{\text{core}} = \mathcal{F}(S_{2n}, S_{1n})$$

Acharya, C.J., Phillips, PLB '13

new experimental input:

$$\langle r_m^2 \rangle_{2n\text{-halo}} - \frac{10}{11} \langle r_m^2 \rangle_{\text{core}} = 3.81^{+0.82}_{-0.71} \text{ fm}^2$$

Togano *et al.* PLB '16



Hammer, CJ, Phillips JPG 44 (2017) 103002

bands: uncertainty from NLO EFT

$$\sim \max \left\{ \frac{\sqrt{mE_{nn}}}{\Lambda}, \frac{\sqrt{mS_{1n}}}{\Lambda}, \frac{\sqrt{mS_{2n}}}{\Lambda} \right\}$$

Correlations in ^{22}C

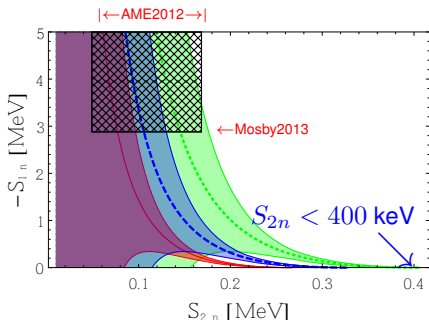
$$\langle r_m^2 \rangle_{2n\text{-halo}} - \frac{A}{A+2} \langle r_m^2 \rangle_{\text{core}} = \mathcal{F}(S_{2n}, S_{1n})$$

Acharya, C.J., Phillips, PLB '13

new experimental input:

$$\langle r_m^2 \rangle_{2n\text{-halo}} - \frac{10}{11} \langle r_m^2 \rangle_{\text{core}} = 3.81^{+0.82}_{-0.71} \text{ fm}^2$$

Togano et al. PLB '16



bands: uncertainty from NLO EFT

$$\sim \max \left\{ \frac{\sqrt{mE_{nn}}}{\Lambda}, \frac{\sqrt{mS_{1n}}}{\Lambda}, \frac{\sqrt{mS_{2n}}}{\Lambda} \right\}$$

Other experimental bound:

- AME2012
 $S_{2n} = 110(60) \text{ keV}$

- Mosby2013
 $-S_{1n} > 2.9 \text{ MeV}$

Hammer, CJ, Phillips JPG 44 (2017) 103002

6 He: $2n$ Halo with p-wave nc interactions

- *ab initio* calculation

- no-core shell model Navrátil *et al.* '01; Sääf, Forssén '14
- NCSM-RGM/Continuum Romero *et al.* '14 '16
- Green's function Monte Carlo Pieper *et al.* '01; '08
- hyperspherical harmonics (EIHH) Bacca *et al.* '12

- Halo EFT in 6 He ground state

- EFT+Gamow shell model (GSM) Rotureau, van Kolck Few Body Syst. '13
- EFT+Faddeev equation C.J., Elster, Phillips, PRC '14;
Göbel, Hammer, CJ, Phillips, Few Body Syst. 60 (2019) 61

- $^{6-10}$ He effective interaction + GSM Fossez, Rotureau, Nazarewicz, PRC '18

P-wave neutron halos

- nc interaction in a p-wave bound/resonance state

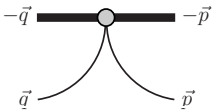
$$\begin{array}{c} n \\ \alpha \end{array} \begin{array}{c} \nearrow \\ \searrow \end{array} = \frac{2\pi}{\mu} \frac{\vec{p} \cdot \vec{q}}{-1/a_1 + r_1 k^2/2 - ik^3}$$

- $a_1 < 0$: shallow resonance: ${}^5\text{He}$ ($3/2^-$)
 - $a_1 > 0$: shallow bound state: ${}^{11}\text{Be}$ ($1/2^-$), ${}^8\text{Li}$ (2^+), ${}^8\text{Li}^*$ (1^+)
- p-wave power counting
 - resum ik^3 : $1/a_1 \sim Q^3$, $r_1 \sim Q$ [Bertulani, Hammer, van Kolck NPA '02]
 - perturbative ik^3 : $1/a_1 \sim Q^2 \Lambda$, $r_1 \sim \Lambda$ [Bedaque, Hammer, van Kolck PLB '03]

Running of 3BF Coupling

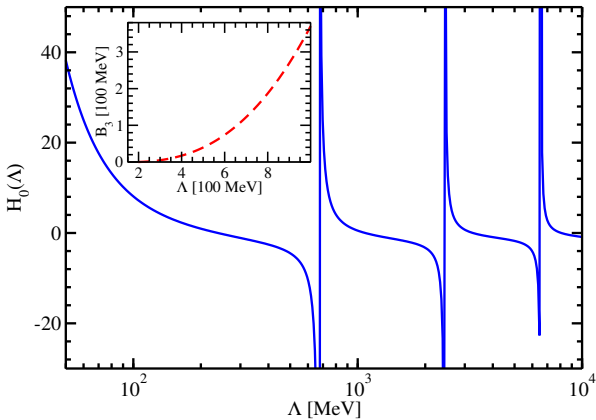
- p-wave 3BF:

reproduce $S_{2n} = 0.973 \text{ MeV}$



$$= M_n \vec{q} \vec{p} \frac{H(\Lambda)}{\Lambda^2}$$

- discrete scaling symmetry is broken due to p-wave interactions



Momentum-space probability density

- The probability density:

$$\rho_i(\mathbf{p}, \mathbf{q}) = \langle \Psi | \mathbf{p}, \mathbf{q} \rangle_i i \langle \mathbf{p}, \mathbf{q} | \Psi \rangle$$

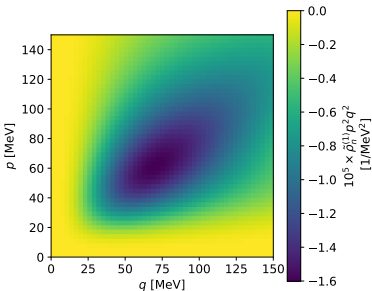
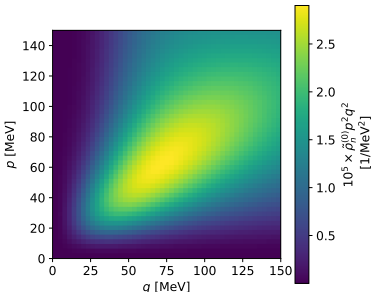
- ℓ th moment (partial-wave decomposition)

$$\rho_i^{(\ell)}(p, q) = \int_{-1}^1 dx P_\ell(x) \rho_i(\mathbf{p}, \mathbf{q})$$

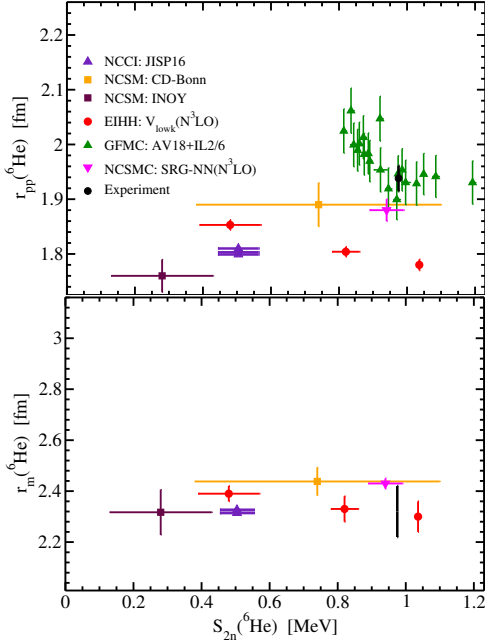
$$x = \frac{\mathbf{p} \cdot \mathbf{q}}{pq}$$

- $\rho_n^{(0)}(p, q)$ and $\rho_n^{(1)}(p, q)$

Göbel, Hammer, CJ, Phillips,
Few Body Syst. 60 (2019) 61



Universal Correlations Among Radii & S_{2n} in ${}^6\text{He}$



• He-6 charge radius
• He-6 matter radius

compare with ab initio calculations

NCCI: Caprio, Maris, Vary, PRC '14

NCSM: Caurier, Navratil, PRC '06

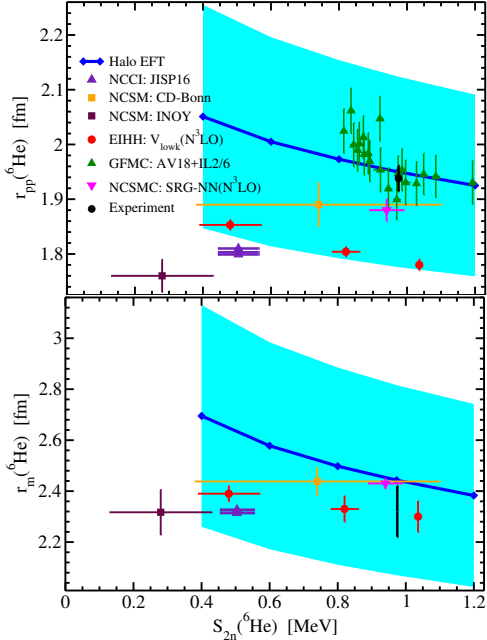
EIHH: Bacca, Barnea, Schwenk, PRC '12

GFMC: Pieper, RNC '08

NCSMC: Romero et al., PRL '16

Halo EFT: preliminary (uncertainty)

Universal Correlations Among Radii & S_{2n} in ${}^6\text{He}$



- He-6 charge radius
- He-6 matter radius

compare with ab initio calculations

NCCI: Caprio, Maris, Vary, PRC '14

NCSM: Caurier, Navratil, PRC '06

EIHH: Bacca, Barnea, Schwenk, PRC '12

GFMC: Pieper, RNC '08

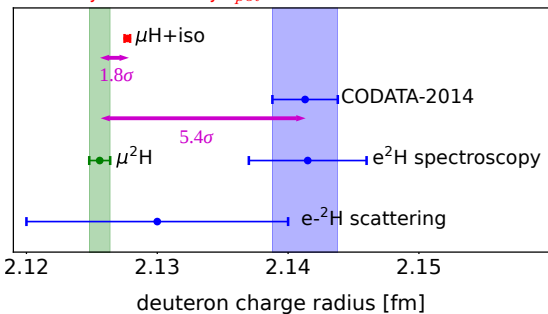
NCSMC: Romero et al., PRL '16

Halo EFT: preliminary (cyan uncertainty)

Nuclear polarization effects in muonic deuterium

- Halo EFT formalism is suitable for study deuteron system (\neq EFT)
- Nuclear polarization δ_{pol} plays crucial role in muonic deuterium Lamb shift
- It is important for the experimental determination of deuteron charge radius

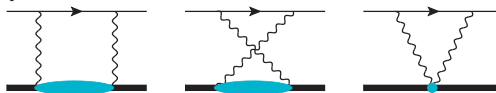
uncertainty dominated by δ_{pol}



deuteron charge radius from Lamb shift in muonic deuterium:
Pohl, et al., Science (2016)

δ_{pol} from virtual Compton tensor

- δ_{pol} is originated in two-photon exchange



- δ_{pol} is dominated by longitudinal response function

$$\delta_{\text{pol}} \propto \iint dq d\omega g(\omega, q) S_L(\omega, q)$$

$$g(\omega, q) = \frac{1}{2E_q} \left[\frac{1}{(E_q - m_\mu)(E_q - m_\mu + \omega)} - \frac{1}{(E_q + m_\mu)(E_q + m_\mu + \omega)} \right]$$

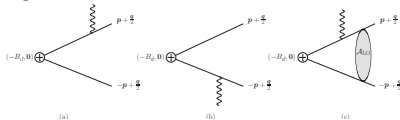
- response function S_L is related to virtual-compton transition matrix elements

$$S_L(\omega, \mathbf{q}) = \int \frac{d^3 p}{(2\pi)^3} \delta \left(\omega - B_d - \frac{q^2}{4m_N} - \frac{p^2}{m_N} \right) \overline{|\mathcal{M}|^2}$$

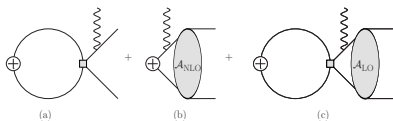
deuteron virtual compton amplitude at NNLO

- compton amplitude is summed to all EM multipolarity

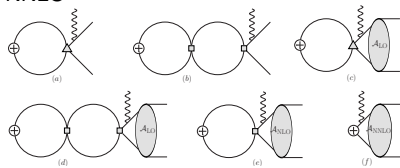
LO



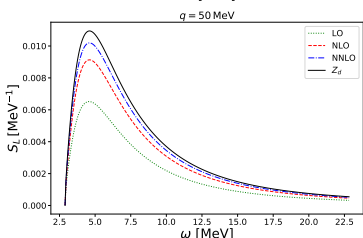
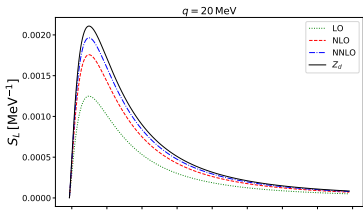
NLO



NNLO



- order-by-order convergence
- 3% accuracy at NNLO



Emmons, CJ, Platter, arXiv:2009.08347

Summary

- Halo nuclei play crucial role in nucleosynthesis, and is important for understanding nuclear astrophysical processes
- Effective field theory comes with limited powers determined by Q and Λ , different EFTs may be efficient at different energy regimes
- Halo EFT describes near-threshold physics in halo nuclei in a controlled expansion in Q/Λ
- Halo EFT rejuvenate cluster models with a systematic uncertainty estimates
- Halo EFT can be connected with *ab initio* calculations
 - adopt inputs from *ab initio* results
 - benchmark with *ab initio* calculations
 - explain correlations among observables in *ab initio* work